Integrating U-net with full-waveform inversion for an efficient salt body construction

Conference Paper · August 2022

DOI: 10.1190/image2022-3751821.1

2 authors:

Abdullah Alali
King Abdullah University of Science and Technology
16 PUBLICATIONS **33** CITATIONS
SEE PROFILE

Tariq Alkhalifah
King Abdullah University of Science and Technology
576 PUBLICATIONS **7,730** CITATIONS
SEE PROFILE

Integrating U-net into full-waveform inversion for an efficient salt body construction

Abdullah Alali[1]*, and Tariq Alkhalifah*[1]
[1]*King Abdullah University of Science and Technology*

SUMMARY

Full waveform inversion (FWI) often faces a lot of difficulty inverting for the subsurface when starting with a poor initial model, especially in complex subsurface regions, such as those containing salt bodies. Thus, human intervention is often needed to pick the salt boundary and improve the starting model for the inversion, which can be erroneous and time consuming. Recently, machine learning has greatly assisted us in interpreting the salt body from seismic images, which helps automate the salt building process. However, such ML algorithms require seismic images, which in turn requires a reasonable good velocity model. Here, we build the salt body using low frequency FWI with the aid of neural networks, specifically U-net. The inversion is implemented in a multi-scale fashion and the networks for flooding and unflooding the salt are applied after each scale. We start the inversion from a constant velocity model using low frequencies of 3-7 Hz. Then, we apply a U-net to improve the inversion and flood the salt. We repeat this process of FWI and flooding in the next frequency bandwidth. In the last frequency bandwidth, we use a U-net for unflooding and impliment a final FWI. The networks were trained in a supervised manner using 1D inverted velocity models. We show the potential of the approach on the center part of BP 2004 salt model.

INTRODUCTION

Full-waveform inversion (FWI) is a powerful technique that reconstructs the unknown velocity of the subsurface by minimizing a misfit between the observed and synthetic data (Tarantola, 1984; Virieux and Operto, 2009). Due to the high oscillatory nature of the seismic data, FWI is prone to cycle-skipping when the synthetic data are far from the observed ones by more than half a cycle, which inevitably traps FWI in a local minimum. Thus, FWI practitioners seek to prevent the cycle-skipping problem by various means. The basic approach is to start the inversion with a good initial model (e.g Alkhalifah, 2016; Alali et al., 2020). In the absence of a good starting model, the low wave-number components, which represent the smooth background, are recovered by a multi-scale approach (Bunks et al., 1995). In the multi-scale approach, different bandwidth of frequencies are used subsequently starting from the low to high frequencies, which corresponds to building the low wave-number components and gradually adding the details to the model.

Applying FWI in complex salt areas requires a prior knowledge of the salt body. The common practice for building the salt is the top-to-bottom workflow. It consists of multiple series of migration and picking the salt's top for flooding, then, migration and picking the salt's base for unflooding Bunks et al. (1995). Flooding refers to smearing the salt's velocity in depth starting from the picked top of the salt, while unflooding refers to removing the excessive flooding beyond the picked base of the salt. The top-to-bottom workflow is labor-intensive, time-consuming and subjective to human interpretation error. Wang et al. (2019); Shen et al. (2017) showed that following the top-to-bottom workflow with FWI can lead to more accurate results provided that the seismic data contain the low frequencies and long offset needed to correct for the salt. In general, building the salt body requires interpreting an initial salt geometry from seismic images and further correction by applying FWI with advanced acquisition such as broadband OBN, long offset, full azimuth and low frequencies recording (Esser et al., 2016; Wang et al., 2019).

The recent advancements in deep learning allowed us to develop algorithms to automate the salt picking process. Convolutional neural networks (CNNs), in particular, are commonly used in object detection and segmentation for their ability to identify image features. A specific CNN architecture, known as U-net (Ronneberger et al., 2015), has achieved high accuracy compared to other architectures in salt detection (Shi et al., 2019; Sen et al., 2020; Naeini et al., 2020).Gramstad and Nickel (2018) proposed to train two CNNs: one to detect the top of the salt for flooding and the other to detect the base for unflooding. Even with these advancements, salt detection during the velocity model building stage is seldom easy due to noise and inaccurate positioning of the reflectors, thus, Zhao et al. (2021) used U-net multiple times in an iterative manner between FWI and reverse time migration (RTM) images. However, a drawback of this approach is that it requires advanced high resolution imaging, which is often expensive. Alali et al. (2022) used U-net to automatically unflood the salt and approximate the subsalt velocity in FWI framework only without applying any imaging by training U-net in a regressive regime. However, they assumed accurate pre-salt sediments and salt flooding.

Here, we extend Alali et al. (2022) implementation by starting without any salt information and a poor initial model. Specifically, we apply FWI starting from a constant velocity model and build the salt body using three networks sequentially: two network for flooding the salt and one to unflood the salt to its base. During the salt building stage, we only use low frequencies in FWI to reduce the cost by allowing coarser grid spacing. We use a 1D U-net for the three networks and generate abundant 1D velocity models for training. We evaluate the performance of our approach on the BP 2004 salt model.

THE METHOD

FWI, in its conventional form, is implemented by minimizing the least square error of the data residual:

$$J_{FWI}(\mathbf{m}) = \left\| \mathbf{d^{obs}} - \mathbf{F}(\mathbf{m}) \right\|_2^2, \tag{1}$$

where $\mathbf{d^{obs}}$ is the observed data, $\mathbf{m}$ is the model, and $\mathbf{F}$ is a forward modelling operator, which is the acoustic constant-density wave equation operator in our case. Starting with a poor initial model (constant below the water bottom), FWI cannot build the salt body using equation 1. Nevertheless, it can reveal some evidence of the salt, such as its initial boundary, probably at the wrong depth (considering the constant initial velocity model). In spite the inaccuracy, such initial information given by the inverted model can be fed to a neural network to predict accurate velocities and Salt granted the network has been trained to do so. Since the process of flooding and unflooding is 1D (Kalita et al., 2019), such training can be performed on 1D synthetic models.

We train three U-net networks: two for flooding and one for unflooding (i.e., U-net1: flooding, U-net2: flooding, U-net3: unflooding) to aid FWI in building the salt model. Naturally, FWI is applied in a multi-scale fashion where we start with low frequency bands and successively include the higher frequencies. Here, after each frequency band, we utilize a network as a post-inversion correction as follow: U-net1 takes the result of the first inversion bandwidth, partly corrects the sediment velocities above the salt, and floods the salt. In the subsequent FWI, we add a total variation regularization (TV) to preserve the flooded salt by U-net1 (Kazei et al., 2017), which reads:

$$\|\mathbf{m}\|_{TV} = |\nabla \mathbf{m}| = \sqrt{\frac{\partial \mathbf{m}}{\partial x} + \frac{\partial \mathbf{m}}{\partial z}}. \tag{2}$$

The subsequent inversions should improve the salt's top dramatically as it starts a with much better model. In the mid-frequency bandwidth, U-net2 is used to apply flooding again in this range as the salt structure and the overall model above the Salt becomes more mature. Finally, U-net3 is applied on the last frequency bandwidth to unflood the salt to its base followed by a final FWI.

THE NEURAL NETWORKS SETUP

We adopt the 1D U-net used in Alali et al. (2022) for all the three networks. It consists of four encoder/decoder blocks and a bottleneck that connects the two parts. Each block consists of two convolutional layers with a batch normalization and a RelU activation function. The size of the input shrinks with each encoding block by a max-pooling operator and increases with each decoder block by a transposed convolutional layer. Each encoder block is connected to its symmetric decoder block with a concatenation operator, which is known as skip connections. The number of channels used in each encoder block starts from 16 and increases by a factor 2 until it reaches 256 in the bottle neck, then, it decreases in a similar fashion in the decoder. A sigmoid function is applied in the last layer to produce the output.

The input for U-net1, U-net2 and U-net3, are FWI results corresponding to the initial frequency band ($\mathbf{m^i_{FWI}}$), mid-frequency band ($\mathbf{m^m_{FWI}}$) and the final frequency band ($\mathbf{m^f_{FWI}}$), respectively. The targets for the flooding network (U-net1 and U-net2) are flooded true models ($m_{flooded}$), while the target for the unflooding network (Unet-3) is the true model ($\mathbf{m_{true}}$). The networks are trained by minimizing the mean square loss (MSE) as follows:

$$\mathbf{L}_{U_1} = \left\| (\mathbf{U1}(\mathbf{m^i_{FWI}}) - \mathbf{m_{flooded}} \right\|_2^2, \tag{3}$$

$$\mathbf{L}_{U_2} = \| (\mathbf{U2}(\mathbf{m^m_{FWI}}) - \mathbf{m_{flooded}} \|_2^2, \tag{4}$$

$$\mathbf{L}_{U_3} = \left\| (\mathbf{U3}(\mathbf{m^f_{FWI}}) - \mathbf{m_{true}} \right\|_2^2. \tag{5}$$

Table 1 shows a summary of the input, output, usage of the three network.

Net	Frequency scale	Input	Output
U-net1	Initial scale	FWI($\mathbf{m_{const}}$)	$\mathbf{m_{flooded1}}$
U-net2	Intermediate scale	FWI($\mathbf{m_{flooded1}}$)	$\mathbf{m_{flooded2}}$
U-net3	Final scale	FWI($\mathbf{m_{flooded2}}$)	$\mathbf{m_{true}}$

Table 1: Summary of the three networks. FWI($\mathbf{x}$) indicates an FWI result starting with $\mathbf{x}$ model.

TRAINING DATASET

To train the three networks, we need to apply tremendous FWI inversions on various possible models. Normally, implementing FWI is expensive, which makes it impractical for generating the necessary number of samples for the training dataset. However, applying FWI on 1D models is much cheaper as it can be implemented using only a single shot (Alali et al., 2022). The flooding and undlooding are naturally applied on the vertical dimension; thus, we implement a 1D FWI on randomly generated 1D models. A prior knowledge of the subsurface is needed to guide the training velocity models distribution so that they somewhat cover what we expect for the target data. Such prior knowledge can come from some wells in the area, or some tomographic velocity. Here, we use the average velocity values of the target area (the BP 2004 salt model) excluding the salt as the background trend in generating the training velocity model samples. We create a total of 10000 random samples. We also randomly include salts with different depth and positions in some of the models. Some of the models are left without salt to teach the network to distinguish between salt or no-salt.

The parameters for modelling the seismic data are as follow: one shot gather with a Ricker wavelet of dominant frequency of 5 Hz, the minimum frequency of the data is 3 Hz and the maximum offset is 15 km. We apply FWI to the generated 1D models starting with a constant velocity equal to that of the water bottom layer and using a data frequency range from 3 to 7 Hz. The results of this inversion form the input to U-net1 and the output is the flooded model. We train the network using a batch size of 32, 100 epochs, and a 0.001 learning rate. The training samples are divided using the common 80/20 split for training and validation, respectively. After training U-net1, it is used to flood all the inverted training samples, which then are used as initial model in a second 1D FWI. Then, we train

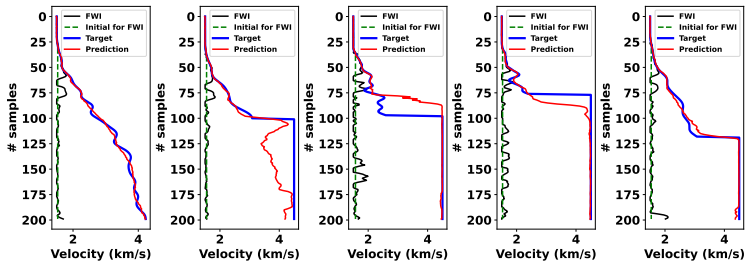

(a)

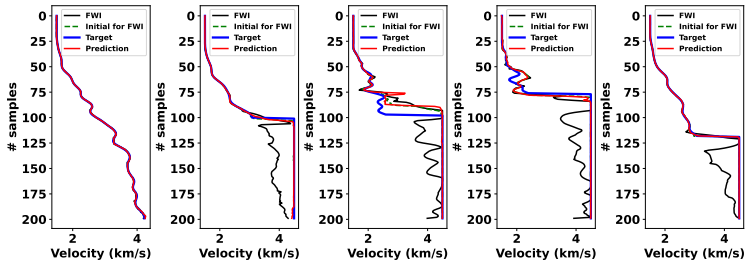

(b)

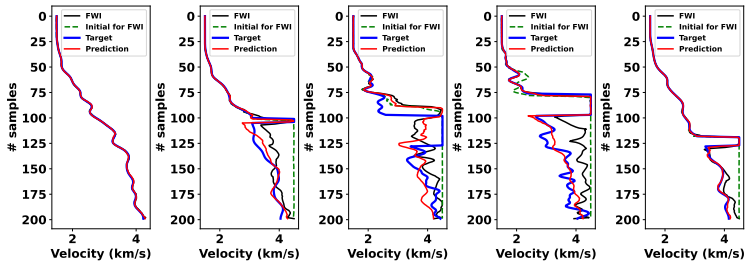

(c)

Figure 1: Samples from the validation set and their corresponding flooding by (a) U-net1, (b) U-net2 and (c) U-net3. The green dashed lines represent the initial models for FWI. The black lines are the inversion results. The red lines represent the network flooding/unflooding using the FWI results (black lines) as inputs to the network and the flooded/true models (blue lines) as the target.

U-net2 with similar hyper-parameters as U-net1. For the unflooding with U-net3, we use the same network as in Alali et al. (2022) without further training as it is trained on the same setup.

Figures 1(a), 1(b) and 1(c) show the performance of the networks U-net1, U-net2 and U-net3, respectively, on five samples from the validation set. Generally, U-net1 improves the inversion result, especially in the first sample, where there is no salt (Figure 1(a)). However, the flooding with U-net1 is not accurate in many cases or incomplete, which suggests the necessity of applying the flooding again. The second flooding with U-net2 (Figure 1(b)) highly improves the result and it corrects the above the salt velocities except for the third samples, which might need another round of FWI and flooding. Figure 1(c) shows the final salt body after the unflooding and a good estimation of the subsalt velocity. Note how the salt was not recovered in the third sample as a result of inaccurate top of the salt. Thus, we advise to repeat the FWI-flooding in a multi-scale approach until we are confident that the salt top is captured well. This can be done cheaply at low frequencies. An interesting observation is that the network increases the resolution of the model although the inversion is implemented with relatively low frequencies. This is courtesy of the networks, which are tasked with injecting high resolution salt information in an otherwise smooth model.

BP 2004 SALT MODEL

We test the trained networks on the center part of the benchmark BP 2004 salt model given in Figure 2. The model is downscaled to half its original size. We synthesize 200 shots placed on the surface with a shot spacing of 66 m. We use a Ricker wavelet of 5 Hz dominant frequency as the seismic source. The data are recorded using 330 receivers placed 40 m apart. The maximum offset is 13.2 km and the minimum frequency is 3 Hz. We apply the multi-scale approach using frequencies from 3 to 7, 10, and 15 Hz. We start the inversion with a constant velocity equal to the water bottom layer of about 1.6 km/s. The first inversion result is shown in Fig-

ure 3(a). The inversion fails to invert the model, which is expected considering our poor initial model. Applying U-net1 to the first inversion result yields Figure 3(b). The network largely improves the background velocity and applies an initial flooding around the salt area. After that, we apply a subsequent FWI in addition to TV using the second frequency bandwidth. The role of TV is to impose edge preserving smoothness in the model and decrease the effect of the lateral discontinuity resulting from the 1D flooding. The result for the second inversion along with its corresponding flooding are plotted in Figure 4. Using only FWI with TV, the salt body is already in a good flooded shape. Applying U-net2 to it improves the flooding and makes the salt sharper. Finally, we apply FWI using the third frequency bandwidth followed by U-net3 for unflooidng. Note, as we are using U-net3 from Alali et al. (2022), we only consider offsets up to 5 km as their network is trained for this setup. The third inversion result with its unflooding are shown in Figure 5. Finally, we apply a final inversion to fine-tune the model and display the result in Figure 6

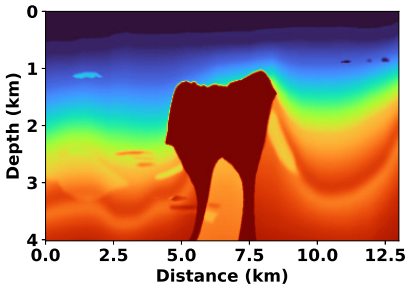

Figure 2: The center part of the BP 2004 salt model.

CONCLUSION

We proposed a method that enabled FWI to reconstruct the salt model starting from a poor initial model by applying multiple flooding and unflooding with U-net networks. Specifically, we train three networks: U-net1 for flooding the salt and improve the initial model, U-net2 for improving the flooding and further correcting the above the salt velocity, and U-net3 to unflood the salt to its base. The networks are implemented between frequency bandwidths in a multi-scale approach. We tested the approach using the center part of a modified BP 2004 salt model. The results shows the potential of the method in building the salt model starting with a poor initial model.

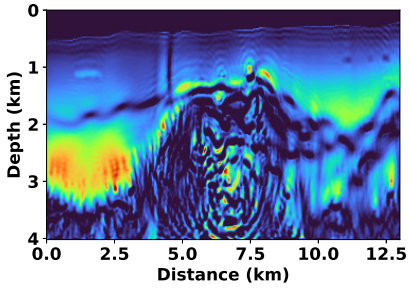

(a)

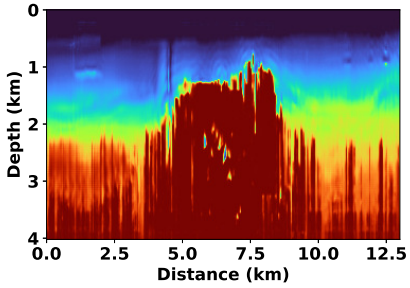

(b)

Figure 3: (a) The first inversion result using frequencies up to 7 Hz and an initial constant velocity model. (b) The flooding using U-net1.

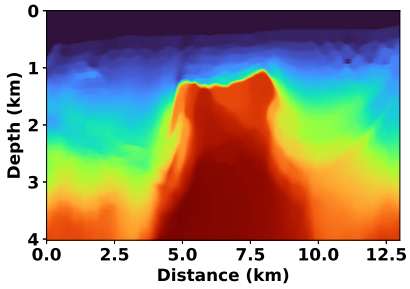

(a)

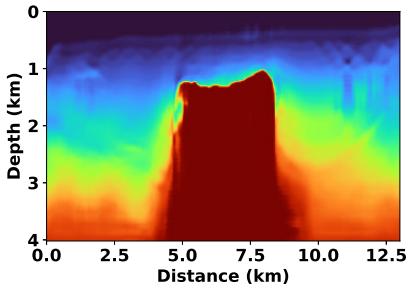

(b)

Figure 4: (a) The second inversion result using frequencies up to 10 Hz and Figure 3(b) as an initial model. (b) The flooding using U-net2.

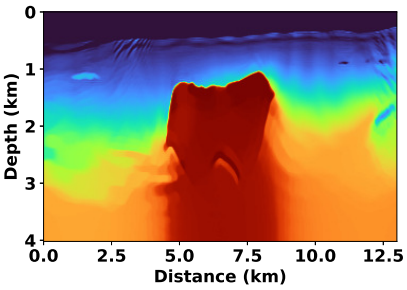

(a)

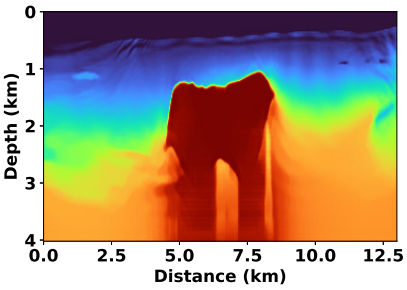

(b)

Figure 5: (a) The third inversion result using frequencies up to 15 Hz and Figure 4(b) as an initial model. (b) The unflooding using U-net3.

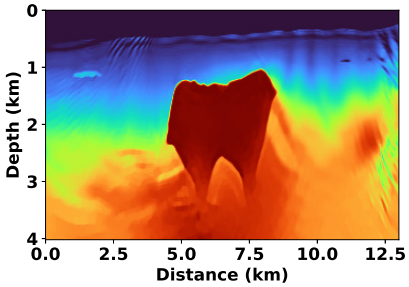

Figure 6: The final inversion using all the frequency bandwidth.

REFERENCES

Alali, A., V. Kazei, M. Kalita, and T. Alkhalifah, 2022, Deep learning unflooding for robust subsalt waveform inversion: Geophysical Prospecting.

Alali, A., B. Sun, and T. Alkhalifah, 2020, The effectiveness of a pseudo-inverse extended born operator to handle lateral heterogeneity for imaging and velocity analysis applications: Geophysical Prospecting, **68**, 1154–1166.

Alkhalifah, T., 2016, Full-model wavenumber inversion: An emphasis on the appropriate wavenumber continuation: Geophysics, **81**, R89–R98.

Bunks, C., F. M. Saleck, S. Zaleski, and G. Chavent, 1995, Multiscale seismic waveform inversion: Geophysics, **60**, 1457–1473.

Esser, E., L. Guasch, F. J. Herrmann, and M. Warner, 2016, Constrained waveform inversion for automatic salt flooding: The Leading Edge, **35**, 235–239.

Gramstad, O., and M. Nickel, 2018, Automated interpretation of top and base salt using deep convolutional networks, *in* SEG Technical Program Expanded Abstracts 2018: Society of Exploration Geophysicists, 1956–1960.

Kalita, M., V. Kazei, Y. Choi, and T. Alkhalifah, 2019, Regularized full-waveform inversion with automated salt flooding: Geophysics, **84**, R569–R582.

Kazei, V., M. Kalita, and T. Alkhalifah, 2017, Salt-body inversion with minimum gradient support and sobolev space norm regularizations: Presented at the 79th EAGE Conference and Exhibition 2017.

Naeini, E. Z., B. Consolvo, P. Docherty, and J. Uwaifo, 2020, Deep learning for salt body detection: A practical approach: 82nd EAGE Annual Conference & Exhibition, European Association of Geoscientists & Engineers, 1–5.

Ronneberger, O., P. Fischer, and T. Brox, 2015, U-net: Convolutional networks for biomedical image segmentation: International Conference on Medical image computing and computer-assisted intervention, Springer, 234–241.

Sen, S., S. Kainkaryam, C. Ong, and A. Sharma, 2020, Saltnet: A production-scale deep learning pipeline for automated salt model building: The Leading Edge, **39**, 195–203.

Shen, X., I. Ahmed, A. Brenders, J. Dellinger, J. Etgen, and S. Michell, 2017, Salt model building at atlantis with full-waveform inversion, *in* SEG Technical Program Expanded Abstracts 2017: Society of Exploration Geophysicists, 1507–1511.

Shi, Y., X. Wu, and S. Fomel, 2019, Saltseg: Automatic 3d salt segmentation using a deep convolutional neural network: Interpretation, **7**, SE113–SE122.

Tarantola, A., 1984, Inversion of seismic reflection data in the acoustic approximation: Geophysics, **49**, 1259–1266.

Virieux, J., and S. Operto, 2009, An overview of full-waveform inversion in exploration geophysics: Geophysics, **74**, WCC1–WCC26.

Wang, P., Z. Zhang, J. Mei, F. Lin, and R. Huang, 2019, Full-waveform inversion for salt: A coming of age: The Leading Edge, **38**, 204–213.

Zhao, T., C. Zhao, A. Kaul, and A. Abubakar, 2021, Automatic salt geometry update using deep learning in iterative fwi-rtm workflows: First International Meeting for Applied Geoscience & Energy, Society of Exploration Geophysicists, 3184–3188.